Supporting Information

Fe doping stabilized γ-Ga_2O_3 thin film with high room temperature saturation magnetic moment

Yuanqi Huang[a,§], Ang Gao[c,§], Daoyou Guo[d], Xia Lu[e,f], Xiao Zhang[a,b], Yalei Huang[d], Jie Yu[a], Shan Li[a], Peigang Li[a,b,*] and Weihua Tang[a,b,*]

[a]*Laboratory of Information Functional Materials and Devices, School of Science, Beijing University of Posts and Telecommunications, Beijing 100876, China*

[b]*State Key Laboratory of Information Photonics and Optical Communications, Beijing University of Posts and Telecommunications, Beijing 100876, China*

[c]*Beijing National Laboratory for Condensed Matter Physics, Institute of Physics, Chinese Academy of Sciences, Beijing 100190, P. R. China*

[d]*Center for Optoelectronics Materials and Devices, Department of Physics, Zhejiang Sci-Tech University, Hangzhou 310018, China*

[e]*School of Materials, Sun Yat-sen University, Guangzhou 510275, China*

[f]*Beijing Advanced Innovation Center for Soft Matter Science and Engineering, Beijing University of Chemical Technology, Beijing 100029, China*

[*]*E-mail addresses: whtang@bupt.edu.cn (Weihua Tang)*

**E-mail: pgli@bupt.edu.cn (Peigang Li)*

[§]Author contributions: Yuanqi Huang and Ang Gao contributed equally.

1. First-principles modeling and calculation details

The net values of spin charge integral at Ga_O, Ga_T and O sites are all zero, revealing that the fully occupied γ-$Ga_{24}O_{32}$ exhibits no FM.

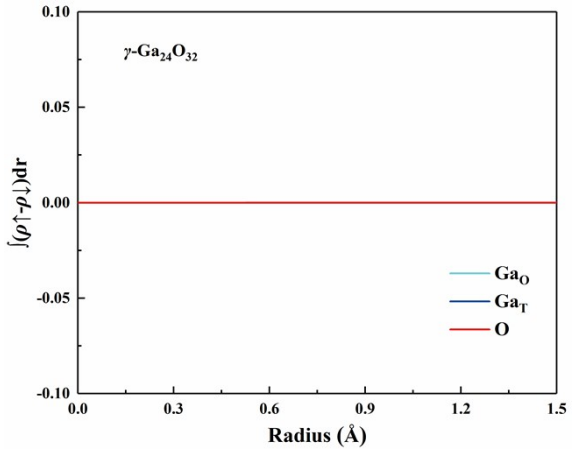

Figure S1. The net spin charge integral of Ga_O, Ga_T and O configurations.

Three cation vacancies that introduced can locate all in the tetrahedral positions (3T), all in the octahedral positions (3O), one in the tetrahedral and two in the octahedral positions (1T2O), or two in the tetrahedral and one in the octahedral positions (2T1O). The calculated formation energy (E_{form}) plotted in Figure S2 suggests that the lowest E_{form} is one of the 2T1O configurations.

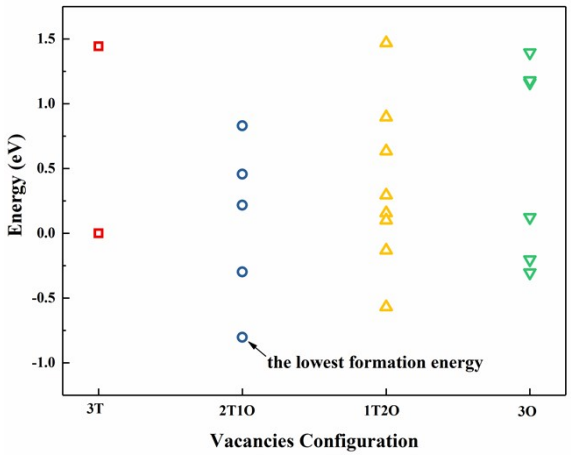

Figure S2. The calculated E_{form} when three cation vacancies take the 3T, 3O, 1T2O, or 2T1O configurations.

Cation vacancies alternately taking the 2T1O configurations (T-O-T) provide the lowest E_{form}. They are long-range orderly distributed along the [111] crystal orientation. The dotted circles in Figure S3b mean that long-range ordered cation vacancies distribute in this vertical direction. Further calculations have verified that such vacancy distribution affects the least on superexchange (not supplied).

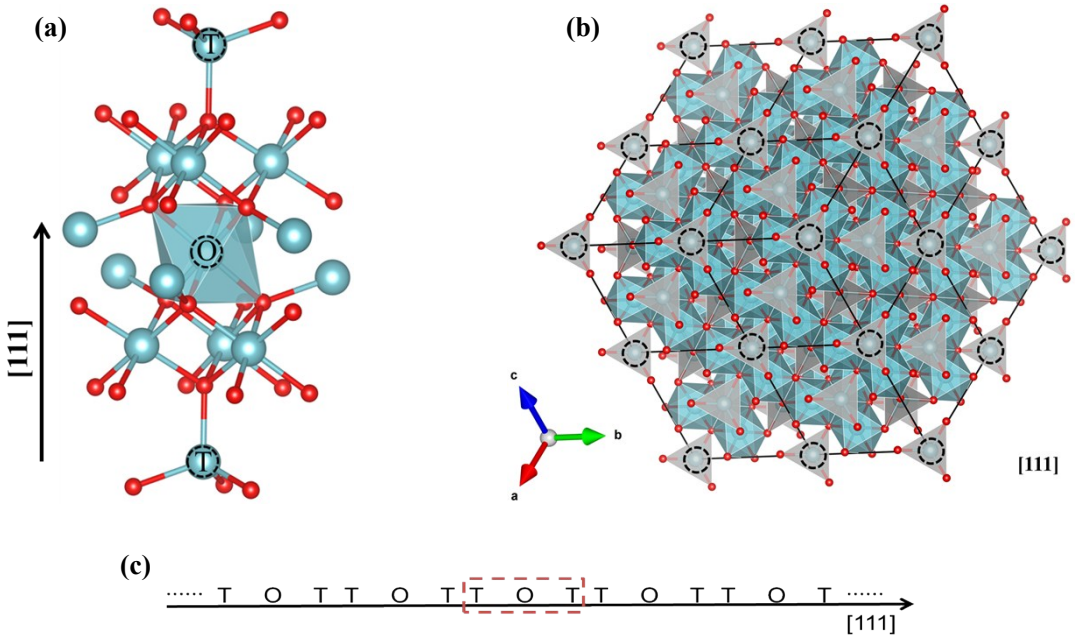

Figure S3. (a) Structural and (c) schematic diagram of the most stable cation vacancy distribution.

(b) Unit cell viewed from [111] direction.

The net spin charge integral values of five distinct Ga positional configurations are calculated. The net values are no longer zero, and weak magnetic moment begins to appear. Through the comparison of Figure S4a and S4b, the magnetism is consisted mainly by Ga configuration which is the nearest to octahedrally coordinative vacancy at position 1. On the contrary, the Ga configuration at position 3 which is the farmost to cation vacancies contributes the lowest. And two tetrahedrally coordinative Ga configurations at position 4 and 5 contribute equally.

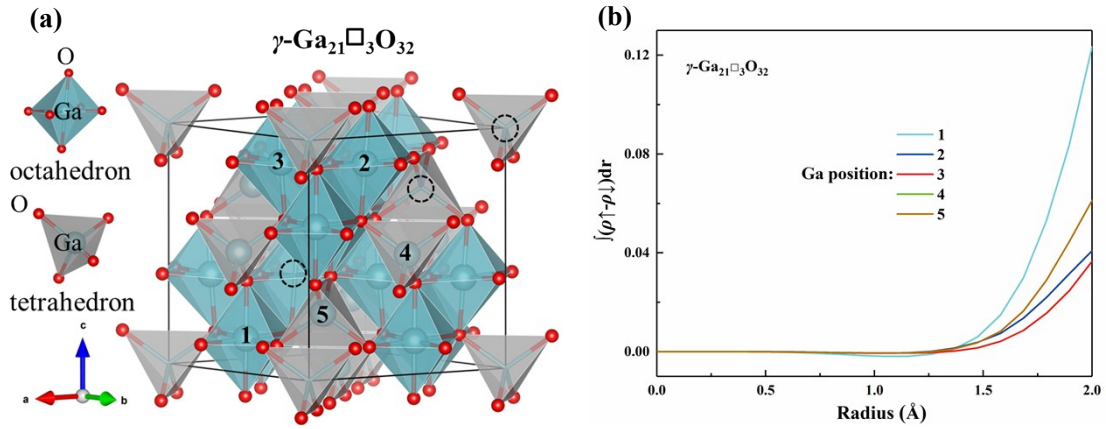

Figure S4. (b) The net spin charge integral of five distinct Ga positional configurations. The occupied sites are labeled in (a).

In γ-$Ga_{21}\square_3O_{32}$ lattice, there are four different Ga configurations where Fe ion could substitute, described as T_1, O_1, O_2 and O_3 in Figure S6a. Herein, the T or O means tetrahedrally or octahedrally coordinative. Meanwhile, high or low spin state is considered. In Figure S6b, it can be concluded that high spin state is significantly more stable than low spin state. Hence, in the following calculations, only high spin state will be considered.

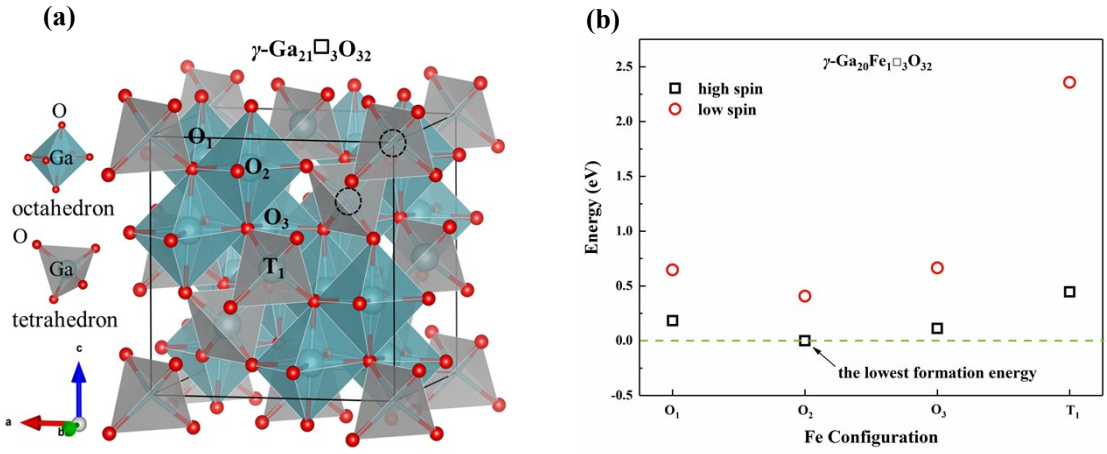

Figure S6. Consider the E_{form} when one Fe atom takes the T_1, O_1, O_2 or O_3 configuration as well as the spin state.

On the basis of the above results, another Fe atom is introduced. While taking into account all the positions and only considering high spin state, the values of E_{form} are shown in Figure S7.

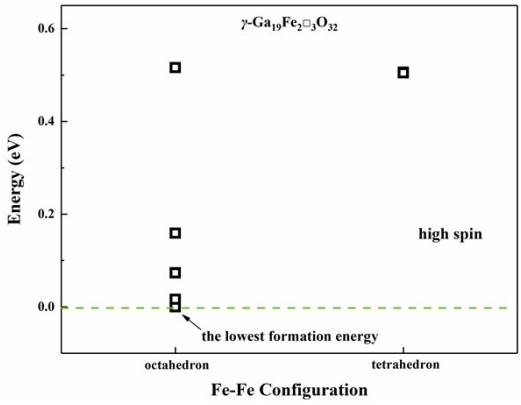

Figure S7. Consider the E_{form} when another Fe atom takes all configurations in high spin state.

2. Supplementary experimental data and interpretation

X-ray pole figure measurements are used to identify phase transformation of Fe doped Ga_2O_3 thin films. According to standard PDF committee data, there should be several diffraction peaks at around 2θ = 30.5° for β-Ga_2O_3, such as (400), (110), (-401), (002) and (-202). However, as for γ-Ga_2O_3, there should be only one peak at around 2θ = 30.5° defined as (220). The reason why these peaks haven't been detected by XRD θ-2θ scan in Figure 3 may be that there is a rotation angle between the preferential orientation and hidden peaks. Hence, in order to detect these planes, we fix the detectors angle of Bruker D8 Discover at 2θ = 30.5°, rotate samples (φ = 0° ~360°) and change the quadrant elevation of the test platform (χ = 0° ~70°). The X-ray pole figures are shown in Figure S5a-S5c. It can be seen that all samples exhibit six-fold symmetry, which is parallel with hexagonal sapphire substrate. For 0 and 5.38 at.% thin films, two sets of diffraction spots at χ = 25° and 55° are detected. Moreover, the spots of 5.38 at.% thin film are more focused and legible, anastomosing with the peak values in Figure 3 and indicating better crystal quality. While for 9.62 at.% thin film, there is only one set of diffraction spots at χ = 35°, which means only one diffraction peak at around 2θ = 30.5°. In order to further confirm these crystal planes, we fix the obtained quadrant elevation χ and rotation angle φ, and then measure the XRD θ-2θ scanning patterns of 0 and 9.62 at.% thin films as shown in Figure S5d. As for 9.62 at.% thin film, when χ = 35°, two peaks at 2θ = 30.64° and 63.43° corresponding to γ(220) and γ(440) are observed. As for pure Ga_2O_3 thin film, when χ = 25°, two peaks at 30.24° and 31.65° which come from β(-401) and β(-202) are tested, respectively. And when χ = 55°, peaks at 29.93° and 43.76° which come from β(002) and β(-112) are

tested, respectively. Theoretically, the inclined angles between β(-201) and β(-401)/β(-202)/β(002)/β(-112) should be 23.48°/22.54°/50.02°/54.33°, which fits well with the actual data. And the inclined angles between γ(111) and γ(220) should be 35.26°, which is also in well consistence with the measured χ. Hence, it can be concluded that we have successfully obtained γ-Ga_2O_3 thin film through doping 9.62 at.% Fe element. Furthermore, measuring the X-ray pole figure in this way can efficiently identify the transformation between β and γ phase Ga_2O_3 without damaging thin films.

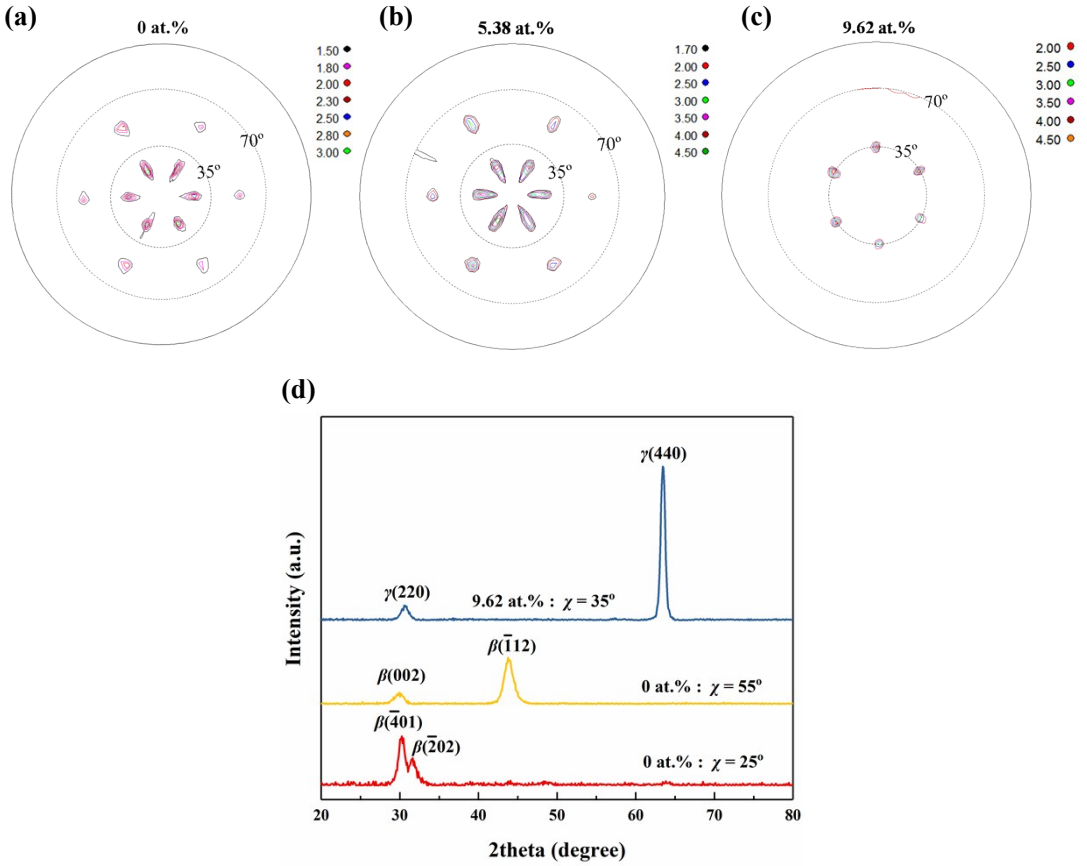

Figure S5. X-ray pole figures of Fe doped Ga_2O_3 thin films with Fe content as (a) 0 at.%, (b) 5.38 at.% and (c) 9.62 at.%, respectively. (d) XRD θ-2θ scanning patterns of thin films with Fe content as 0 and 9.62 at.%.

To understand the underlying mechanism of phase transition, XPS measurements are used to test the element binding and valence in thin films. The spectrum charge-shift is calibrated using the fortuitous C 1*s* peak at 284.8 eV. Figure S8a presents the XPS spectrum with the binding energy in range of -10 ~ 1210 eV. The determined XPS peaks of Ga and O are indicated in all curves, and extra Fe element is discovered in Fe doped samples. No other elements are detected from wide scan spectra, indicating the obtaining of high purity Ga_2O_3:Fe thin films. From Figure S8b, two symmetrical peaks of Ga $2p_{1/2}$ and Ga $2p_{3/2}$ located at 1145.2 eV and 1118.3 eV for β-

Ga_2O_3, 1145.1 eV and 1118.2 eV for β-Ga_2O_3:Fe, 1144.5 eV and 1117.5 eV for γ-Ga_2O_3:Fe thin films are obtained. The separation distances between these two peaks are all about 26.9 eV, which is in good agreement with the binding energy of Ga 2*p* (Δ = 26.8 eV). For γ phase, there is an obvious blue shift of Ga 2*p* binding energy, indicating that the bonding form of the Ga-O bond has changed. Figure S8c shows the Fe 2*p* core levels of β-Ga_2O_3:Fe and γ-Ga_2O_3:Fe thin films. Also, there is a red shift of Fe 2*p* binding energy for γ phase as compared with β phase, indicating that the bonding form of the O-Fe bond has changed. In one hand, these shifts can be contributed to different Ga-O-Fe bonds because of the phase transition, which may be an intrinsic difference in these two phases.[76] In the other hand, these shifts demonstrate that the charge transfer contribution changes with the increase of Fe concentration and phase transition.[77, 78] Normally, as for Fe^{3+} cation, the peak positions of Fe $2p_{1/2}$ and Fe $2p_{3/2}$ are located at about 724.6 and 711.0 eV. While as for Fe^{2+} cation, the peak positions of Fe $2p_{1/2}$ and Fe $2p_{3/2}$ are located at about 722.6 and 709.0 eV. Herein, the Fe $2p_{1/2}$ and Fe $2p_{3/2}$ are located at 723.3 eV and 709.5 eV for β phase, and 723.6 eV and 709.8 eV for γ phase, respectively. They are located between the values of Fe^{3+} and Fe^{2+} ions, meaning the coexistence of Fe^{3+} and Fe^{2+}. Hence, the Fe $2p_{3/2}$ core level can be separated into two peaks defined as Fe^{3+} (peak I) and Fe^{2+} (peak II). The ratios of Fe^{3+}/Fe^{2+} for β- & γ-Ga_2O_3:Fe thin films are 1.16 & 1.93, respectively. Theoretically, with Fe ([Ar]$3d^6 4s^2$) dopants, the extra electrons introduced by oxygen vacancies would enter the Fe *d*-shell, leading to the neutral acceptors (Fe^{3+}) converts to negatively charged acceptors (Fe^{2+}), and this process may suppress the unintentional extra carriers. In another word, the Fe^{2+} content is bound up with the oxygen vacancy in thin films. The ratio of Fe^{3+}/Fe^{2+} for β phase is lower than that of γ phase, which means the proportion of oxygen vacancies in γ phase might be more. In Figure S8d, O 1*s* core level can be divided into two components (I and II) to qualitatively and semi-quantitatively evaluate the amount of oxygen vacancies. The main peak I could be assigned to the oxygen in Ga_2O_3 lattice, while the peak II is usually associated with the oxygen vacancy, C/O bond and OH^- related to carbonaceous contamination. Herein, the peak area ratios I/II are 7.99 for β-Ga_2O_3, 8.48 for β-Ga_2O_3:Fe, and 1.85 for γ-Ga_2O_3:Fe thin films, respectively. It is apparently that the proportion of oxygen defects is comparatively more in Fe doped γ-Ga_2O_3 thin film.

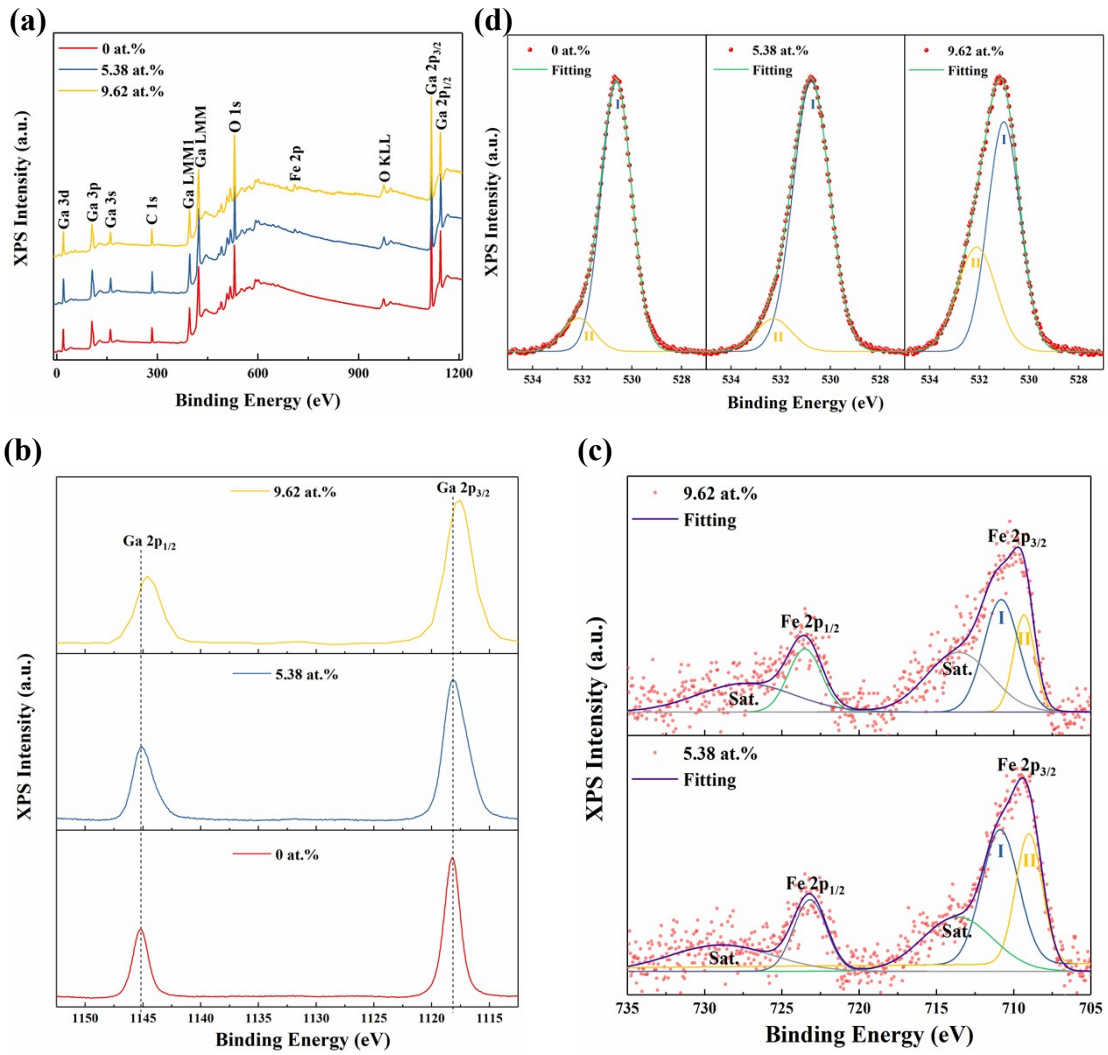

Figure S8. XPS (a) survey spectrum, (b) Ga 2*p*, (c) Fe 2*p* and (d) O 1*s* core levels spectra of Fe doped Ga_2O_3 thin films with different Fe content.

Figure S9 shows the UV-vis absorption spectrum of Fe doped Ga_2O_3 thin films with different Fe content. The host curve exhibits a sharp absorption edge at around 250 nm, whilst the curves with Fe doping display clear blue shift. It is evident that Fe doping increases the transmittance at the range of 260~800 nm. Besides, it can be seen that the UV-vis absorption spectrum of β-Ga_2O_3:Fe and γ-Ga_2O_3:Fe thin films are similar. However, there still exists difference between them. For instance, the γ-Ga_2O_3:Fe thin film exhibits a broader Urbach band tail below the optical band edge, which is commonly associated with more defects.[79] Experientially, the BG energy will increase systematically with the decrease of thickness,[80, 81] the decrease of lattice constant,[82] excess oxygen[83] and nonlinearly vary with crystalline quality[84]. Herein, compared with β-Ga_2O_3:Fe thin film, γ-Ga_2O_3:Fe thin film owns thicker thickness, larger lattice constant, higher O/Ga ratio and lower crystalline quality, resulting in the similarity on the UV-vis absorption spectrum with β phase. The relationship between the optical absorption coefficient (α) and the photon energy ($h\upsilon$) can be expressed as

$$(\alpha h\upsilon)^2 = B\ (h\upsilon - E_g)$$

Where B is a constant, and E_g is the optical BG energy of the materials, which can be obtained through fitting the linear region of the $(\alpha h\upsilon)^2$ versus $h\upsilon$ plot shown by the inset in Figure S9. The E_g is 5.00 eV, 5.12 eV and 5.11 eV for β-Ga_2O_3, β-Ga_2O_3:Fe and γ-Ga_2O_3:Fe thin films, respectively. The large BG provides high photon energy as well as high transparency in the visible and ultraviolet regions (> 280 nm), which makes the manipulation of the spins by photons easier in Fe doped Ga_2O_3 thin films.

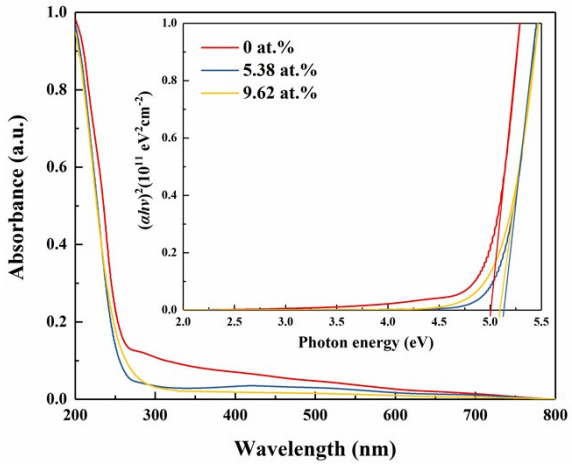

Figure S9. UV-vis absorbance spectrum of Fe doped Ga_2O_3 thin films with different Fe content and the plot of $(\alpha h\upsilon)^2$ versus $h\upsilon$ in inset.

Figure S10 shows the surface morphology image of Fe doped γ-Ga_2O_3 thin film for a 2 × 2 μm^2 scanning area. The mean surface roughness (Ra) is 83.9 pm, and the root mean square roughness (Rq) is 107.0 pm. As the thin film has a thickness of about 203 nm, it implies a smooth surface.

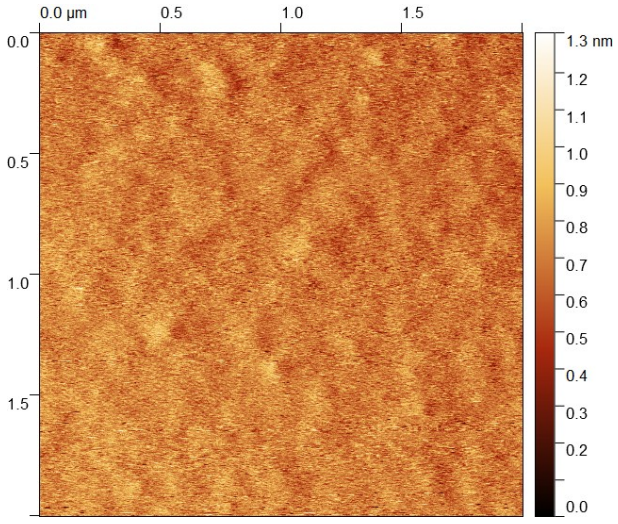

Figure S10. Surface morphology of the Fe doped γ-Ga_2O_3 thin film.

3. Supplementary Tables

Table S1. The magnetic parameters of Fe doped Ga_2O_3 thin films.

Fe content (at.%)	M_s (μB/Fe)	M_r (emu/cm^3)	Coercivity (Oe)
5.38	2.20	3.59	36.62
9.62	5.73	14.37	40.71

It is well-known that γ phase is always metastable (> 650 ºC) and hard to fabricate. Doping technology is a practical approach to obtain thermostable γ-Ga_2O_3 thin film at high temperature.[21] There are two main reasons: a) Due to the ion radii difference, the replacement of Fe^{2+} and Fe^{3+} ions for Ga^{3+} ions will induce a slight lattice expansion, leading to a further phase transition.[85] b) Doping process may reduce the E_{form} and result in a more stable system, supporting phase stability at high temperature.[86] The values of calculated E_{form} in Table S2 provide favorable evidence for phase stabilization. While doping Fe in γ-$Ga_{21}\square_3O_{32}$, the reduced E_{form} is always higher than that in β-$Ga_{24}O_{36}$, wherever substituting at Ga_O or Ga_T site. Qualitatively, it reveals that Fe doping process is beneficial to reduce the total E_{form} of γ phase and stabilize this metastable phase at the high temperature of 750 ºC.

Table S2. The reduced E_{form} of doping Fe in β/γ-Ga_2O_3 at octahedral or tetrahedral sites.

Types	Doping-Fe_O	Doping-Fe_T
β-$Ga_{24}O_{36}$	-0.28 eV	-1.86 eV
γ-$Ga_{21}\square_3O_{32}$	-2.34 eV	-1.89 eV

4. Supplementary Explanation

E1. The origin of the RT ferromagnetic property in Fe doped β-Ga_2O_3 thin film.

Since the XRD and XPS measurements have confirmed the successful substitution of Fe for Ga and ruled out the possible secondary phases of Fe metal cluster and Fe-based oxides. It is reasonable to conclude that the RT ferromagnetism in the β-Ga_2O_3:Fe thin film is intrinsic.[87] The RT ferromagnetism of β-Ga_2O_3:Fe thin film can be ascribed to the following two origins: a) According to Figure S8 (d), there exist a lot of oxygen vacancies in β-Ga_2O_3:Fe thin film. The oxygen vacancy defects will overlap many Fe ions to yield bound magnetic polarons (BMPs), which results in FM coupling between the Fe ions.[64] b) Although there may not exist lots of Ga vacancies in β-Ga_2O_3 thin film like defective γ phase. Coexistence of Fe^{2+} and Fe^{3+} ions also provide a reservoir of charge carriers. According to CT ferromagnetism

model, in which charge transfer from the reduced form of Fe ions to the local density of states associated with extended structural defects leads to the asymmetry of spin.[65]